SCIENTIFIC REPORTS

OPEN

Toll-like receptor 7 deficiency protects apolipoprotein E-deficient mice from diet-induced atherosclerosis

Received: 17 November 2016
Accepted: 20 March 2017
Published online: 12 April 2017

Cong-Lin Liu[1,2], Marcela M. Santos[2], Cleverson Fernandes[2], Mengyang Liao[2], Karine Iamarene[2], Jin-Ying Zhang[1], Galina K. Sukhova[2] & Guo-Ping Shi[1,2]

Toll-like receptor 7 (TLR7) mediates autoantigen and viral RNA-induced cytokine production. Increased TLR7 expression in human atherosclerotic lesions suggests its involvement in atherogenesis. Here we demonstrated TLR7 expression in macrophages, smooth muscle cells (SMCs), and endothelial cells from mouse atherosclerotic lesions. To test a direct participation of TLR7 in atherosclerosis, we crossbred TLR7-deficient (*Tlr7*$^{-/-}$) mice with apolipoprotein E-deficient (*Apoe*$^{-/-}$) mice and produced *Apoe*$^{-/-}$ *Tlr7*$^{-/-}$ and *Apoe*$^{-/-}$ *Tlr7*$^{+/+}$ littermates, followed by feeding them an atherogenic diet to produce atherosclerosis. Compared to *Apoe*$^{-/-}$ *Tlr7*$^{+/+}$ mice, *Apoe*$^{-/-}$ *Tlr7*$^{-/-}$ mice showed reduced aortic arch and sinus lesion areas. Reduced atherosclerosis in *Apoe*$^{-/-}$ *Tlr7*$^{-/-}$ mice did not affect lesion macrophage-positive area and CD4^{+} T-cell number per lesion area, but reduced lesion expression of inflammatory markers major histocompatibility complex-class II and IL6, lesion matrix-degrading proteases cathepsin S and matrix metalloproteinase-9, and systemic serum amyloid A levels. TLR7 deficiency also reduced aortic arch SMC loss and lesion intima and media cell apoptosis. However, TLR7 deficiency did not affect aortic wall elastin fragmentation and collagen contents, or plasma lipoproteins. Therefore, TLR7 contributes to atherogenesis in *Apoe*$^{-/-}$ mice by regulating lesion and systemic inflammation. A TLR7 antagonist may mitigate atherosclerosis.

Toll-like receptors (TLRs) are pattern recognition receptors that recognize distinct evolutionarily conserved structures on pathogens, termed pathogen-associated molecular patterns (PAMPs) and play essential roles in innate immunity[1,2]. Recent studies suggest an involvement of TLRs in atherosclerosis[3–5]. However, the role of TLRs in atherosclerosis has been controversial. TLR3 and TLR4 activation promoted atherosclerosis[6]. Deficiency of TLR2, TLR3, and TLR4 protected low-density lipoprotein receptor-deficient (*Ldlr*$^{-/-}$) mice[6–9] and apolipoprotein E-deficient (*Apoe*$^{-/-}$) mice[10] from atherosclerosis. However, these TLRs have also been suggested to play protective roles in murine atherosclerosis. TLR4 signaling protected *Apoe*$^{-/-}$ mice from periodontal pathogen-induced atherosclerosis[11]. In *Apoe*$^{-/-}$ mice, TLR3 deficiency accelerated the onset of atherosclerosis[12]. Absence of TLR9 also protected *Apoe*$^{-/-}$ mice from spontaneous atherosclerosis[13].

While TLR2 and TLR4 are localized on cell surface, TLR3, TLR7, and TLR9 are localized to the endolysosomal membrane where these TLRs mediate autoantigen and bacterial and viral nucleic acid infection-induced inflammatory cytokine production. For example, viral single-strand RNA (ssRNA) binding on TLR7[14] is required for B cell proliferation, and such activity of TLR7 is specific for RNA-containing antigens[15]. TLR stimulation by microbial infection results in elevated production of IL6 and other cytokines that block regulatory T-cell *de novo* generation[16] and function[17], which play protective roles in atherosclerosis[18,19]. The role of TLR7 in atherosclerosis has also been controversial. In normal human arteries, including aorta, carotid, iliac, mesenteric, subclavian, and temporal, there was negligible expression of TLR7[20]. However, human atherosclerotic lesions contained elevated levels of TLR7[21], suggesting an involvement of TLR7 in atherosclerosis. TLR7 signaling is mediated by MyD88, which activates downstream interferon regulatory factor 5 (IRF5) and IRF7 for the production of inflammatory

[1]Department of Cardiology, Institute of Clinical Medicine, the First Affiliated Hospital of Zhengzhou University, Zhengzhou, China. [2]Department of Medicine, Brigham and Women's Hospital and Harvard Medical School, Boston, MA, 02115, USA. Cong-Lin Liu and Marcela M. Santos contributed equally to this work. Correspondence and requests for materials should be addressed to G.-P.S. (email: gshi@rics.bwh.harvard.edu)

cytokines (e.g. IL6 and TNF-α) and type I interferon (e.g. IFN-α), respectively[22]. In a femoral artery cuff placement-induced neointima thickness model in hypercholesterolemic ApoE*3-Leiden mice, TLR7 expression was increased 14 days after the surgery. Blocking of TLR7 signaling with its antagonist reduced neointimal formation, luminal stenosis, and foam cell formation by greater than 60% with concurrent reduction of arterial wall macrophage infiltration. Stimulation of macrophages with the TLR7 ligand imiquimod enhanced TNF-α expression[23]. Similar observations were obtained in collar placement-induced carotid artery atherosclerosis-like lesion development in hypercholesterolemic rabbits. TLR7 activation with imiquimod increased carotid artery lesion intima area, lipid deposition, and lesion macrophage and lymphocyte contents[24]. However, primary cultured human aortic wall endothelial cells (ECs) and smooth muscle cells (SMCs) produced chemokines IL8 and E-selectin in responding to ligands of TLR3 (Poly I:C), TLR4 (lipopolysaccharide), and TLR5 (flagellin), but do not respond to TLR7 ligand ssRNA[25]. In $Apoe^{-/-}$ mice fed a chow diet, TLR7 deficiency increased aortic root atherosclerotic lesion area and lesion macrophage accumulation, with reduced lesion SMC and collagen contents. In the peripheral blood, TLR7 deficiency led to increased plasma monocyte chemoattractant protein-1 (MCP-1) and increased inducible nitric oxide synthase (iNOS)-positive M1 macrophage contents. Macrophages from these mice also produced more MCP-1, TNF-α, IL6, and IL10 after stimulation with a TLR2 ligand lipoteichoic acid[21]. In lupus-prone $Fasl^{gld/gld}Apoe^{-/-}$ mice, deficiency of IRF5 increased aortic root and arch lesion area and plasma levels of triglyceride, cholesterol, phospholipids, and non-esterified fatty acids, with concurrent reduction of plasma IL10 levels. Bone marrow macrophages from IRF5-deficient mice also showed reduced IL10 production in response to TLR7 ligands R848 or R837[26]. Therefore, the exact role of TLR7 in atherosclerosis remains uncertain and may depend on different experimental model systems.

In this study, we used TLR7-deficient ($Tlr7^{-/-}$) mice and atherogenic diet-fed $Apoe^{-/-}$ mice to test whether TLR7 deficiency affects atherogenesis differently from $Apoe^{-/-}$ mice not on an atherogenic diet or mice on a $Fasl^{gld/gld}$ lupus background.

Materials and Methods

Mice and experimental model. Both $Apoe^{-/-}$ mice (C57BL/6, N = 15, #002052) and $Tlr7^{-/-}$ mice (C57BL/6, N > 10, #008380) were purchased from the Jackson Laboratory (Bar Harbor, ME, USA) and crossbred to generate $Apoe^{-/-}$ $Tlr7^{-/-}$ mice and $Apoe^{-/-}$ $Tlr7^{+/+}$ littermates. Eight to ten-week-old male mice were used to induce atherosclerosis by feeding mice a high cholesterol (1.25%) atherogenic diet (#D12108c, Research Diets Inc. New Brunswick, NJ). After 3 months on this diet, mice from both groups were sacrificed with carbon dioxide narcosis, followed by cardiac puncture blood collection, heart and aortic arch tissue harvest. Aortic root was prepared by cutting away about 70% of the ventricles, and embedding the up portion of the heart that contained the aortic root in optimum cutting temperature (OCT) for sectioning as described previously[27]. Six μm aortic root sections were prepared for oil-red O (ORO) staining to determine atherosclerotic lesion sizes. To analyze atherosclerotic lesion in the aortic arch, we used longitudinal sections from the whole arch embedded in OCT. We collected only sections that contained all three branches (brachiocephalic artery, left common carotid artery, and left subclavian artery) as we reported[28]. Aortic arch sections were also stained with ORO to determine atherosclerotic lesion sizes. We can typically cut 8–10 serial numbered slides (3 sections per slide) and select for each staining the slides with the same lesion location, which corresponds to the same slide serial number. For example, we used one serial numbered slide for Mac-3, CD4, and major histocompatibility complex class II (MHC-II) for all mice, and used another same serial numbered slides from all mice for ORO staining. This approach gives central location of each lesion in each aortic arch with the maximal comparability of quantitative data. All animal procedures conformed to the Guideline for the Care and Use of Laboratory Animals published by the US National Institutes of Health and were approved by the Harvard Medical School Standing Committee on Animals (protocol # 03759).

Immunohistological analysis. Serial aortic arch cryostat cross-sections were used for immunostaining to detect TLR7 (1:150, #ab45371, Abcam, Cambridge, MA), macrophages (Mac-3, 1:900, #553322, BD Biosciences, San Jose, CA), $CD4^+$ T cells (CD4, 1:90, #553043, BD Biosciences), MHC-II (1:250, #556999, BD Biosciences), elastin (Modified Verhoeff Van Gieson Elastic Stain Kit, #HT25A-IKT, Sigma-Aldrich, St. Louis, MO), collagen (0.1% Sirius Red; #09400, Polysciences Inc., Warrington, PA), SMC (α-actin, 1:750, #F3777, Sigma-Aldrich), IL6 along with rabbit IgG isotype (IL6, 1:50, #ab6672, Abcam), IL4 (IL4, 1:50, #ab11524, Abcam), TGF-β (1:300, #sc-146, Santa Cruz Biotechnologies, Inc, Dallas, TX), TLR2 (1:50, #ab1655, Abcam, Cambridge, MA), cathepsin S (CatS) (1:100)[29], and matrix metalloproteinase-9 (MMP-9) (1:400, #AB804, Chemicon International, Temecula, CA). Apoptotic cells in lesions were determined with the *in situ* apoptosis detection kit according to the manufacturer's instructions (#S7100, Millipore, Billerica, MA). Immunostained slides were visualized with either the liquid diaminobenzidine (DAB) substrate chromogen system (#K3468, DAKO, Carpinteria, CA) and counter-stained with methyl green (#H-3402, Vector Laboratories, Inc, Burlingame, CA) (TGF-β, IL-4, IL-6, and TLR7), or with 3-amino-9-ethyl carbazole (#K3464, AEC) (DAKO) and counter-stained with Gill's hematoxylin solution (GHS316, Sigma-Aldrich) (macrophage, MHC-II, $CD4^+$ T cell and SMC). Elastin degradation, collagen content, and media SMC accumulation were graded according to the grading keys that were described previously[30,31]. $CD4^+$ T cells and TUNEL-positive apoptotic cells were counted manually in a blinded fashion and presented as numbers per aortic section. Images of the relative macrophage, MHC-II, IL6, IL4, and TGF-β contents within the aortas were captured by a Microscope VS120 Whole Slide Scanner (Olympus) and quantified by measuring the immunostaining signal-positive areas using computer-assisted image analysis software (Image-Pro Plus; Media Cybernetics, Bethesda, MD). All mouse experiments were performed, and data were analyzed in a blinded fashion by at least two observers.

Immunofluorescent double staining. Cell type (macrophage, SMC, and EC)-specific expression of TLR7 in mouse atherosclerotic lesions was determined by immunofluorescent double staining using rabbit anti-mouse

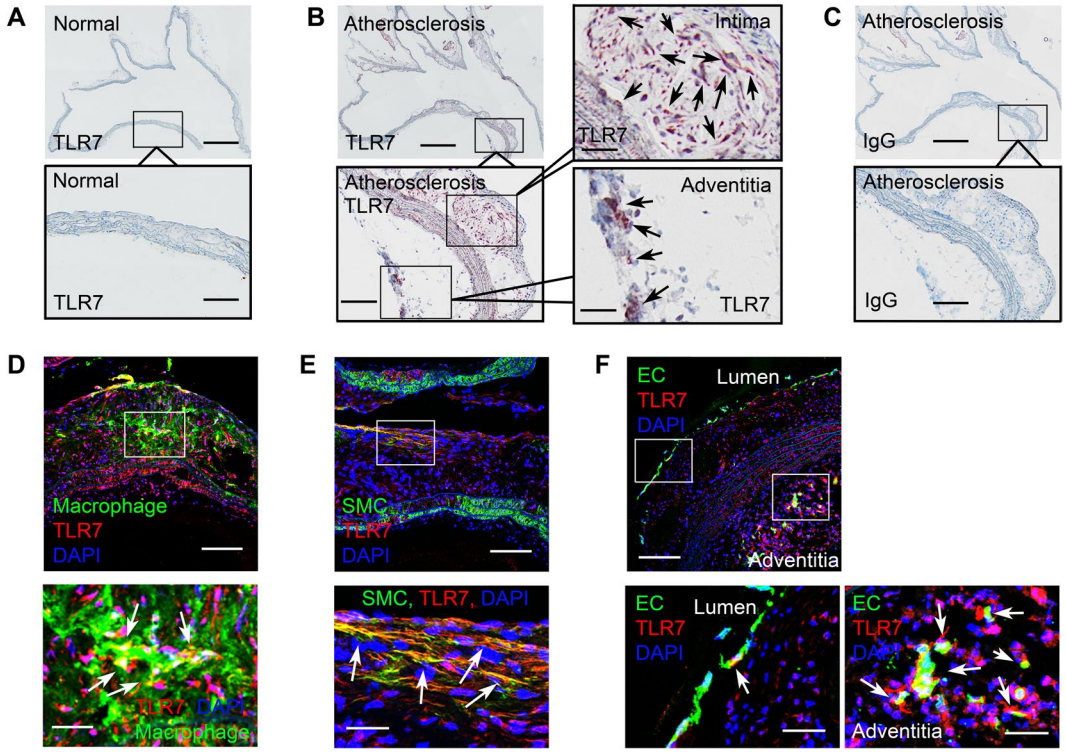

Figure 1. TLR7 expression in mouse atherosclerotic lesions. (**A**) Rabbit-anti-mouse TLR7 monoclonal antibody immunostaining of a normal mouse aortic arch. Scale: 1 mm, inset scale: 200 μm. (**B**) Rabbit-anti-mouse TLR7 monoclonal antibody immunostaining of an aortic arch from an *Apoe*$^{-/-}$ mouse with atherosclerosis showed TLR7 expression in intima and adventitia. Scale: 1 mm, inset scales: 200 and 68 μm. Arrows indicate TLR7-positive cells. (**C**) Rabbit IgG isotype immunostaining of a parallel aortic arch from an *Apoe*$^{-/-}$ mouse with atherosclerosis. Scale: 1 mm, inset scale: 200 μm. (**D–F**) Immunofluorescent double staining of mouse aortic arch atherosclerotic lesions with antibodies against TLR7 and cell type markers (Mac-2, α-actin, and CD31) for macrophage, SMC, and EC from both the lumen and adventitia microvessels. Scale: 100 μm, inset scale: 25 μm. Arrows in the insets indicate TLR7-positive macrophages (**D**), SMCs (**E**), and ECs in lumen and adventitia (**F**).

TLR7 monoclonal antibody (1:100, ab45371, Abcam) together with rat anti-mouse Mac-2 monoclonal antibody (macrophages, 1:100, CL8942AP, CEDARLANE, Burlington, NC), purified rat anti-mouse CD31 monoclonal antibody (EC, 1:900, #553370, BD Biosciences), and FITC-conjugated mouse anti-α-smooth muscle actin monoclonal antibody (SMC, 1:500, F3777, Sigma-Aldrich). Mouse aortic arch lesion macrophage and SMC apoptosis was also detected by immunofluorescent double staining with Alexa Fluor® 594-conjugate cleaved caspase-3 (Asp175) (D3E9) rabbit monoclonal antibody (1:200, #8172, Cell Signaling Technology, Danvers, MA) together with rat anti-mouse Mac-2 monoclonal antibody or FITC-conjugated mouse anti-α-smooth muscle actin monoclonal antibody as mentioned above. Images were collected under an Olympus FluoView™ FV1000 Confocal Microscope.

Plasma protein measurements. Mouse plasma was collected after mice were fasted overnight and stored at −80 °C until analysis. Plasma IL6 (#88-7064-88), IFN-γ (#88-7314-88) (eBioscience, Inc., San Diego, CA), and serum amyloid A (SAA) (#MSAA00, R&D Systems, Minneapolis, MN) levels were determined using ELISA kits according to the manufacturers' instructions. Plasma total cholesterol, triglyceride, and high-density lipoprotein (HDL) levels were determined using reagents from Pointe Scientific (Canton, MI) and the level of low-density lipoproteins (LDL) was calculated as the following formula: LDL = total cholesterol − HDL − (triglycerides/5) as previously reported[32]. Investigators were blinded to the sources of samples during the assays.

Statistical analysis. All mouse data were expressed as mean ± SEM. Due to our small sample sizes and often skewed data distributions, we performed a pairwise non-parametric Mann-Whitney test followed by Bonferroni corrections to examine the statistical significances. SPSS 16.0 was used for analysis.

Results

TLR7 expression in mouse atherosclerotic lesions. Prior studies revealed elevated TLR7 expression in human atherosclerotic lesions[21], but negligible TLR7 in normal human arteries[20]. We obtained similar observations in mouse atherosclerotic lesions. TLR7 immunostaining did not detect TLR7 expression in normal mouse aorta (Fig. 1A). In contrast, rabbit anti-mouse TLR7 antibody revealed elevated TLR7 expression in the intima

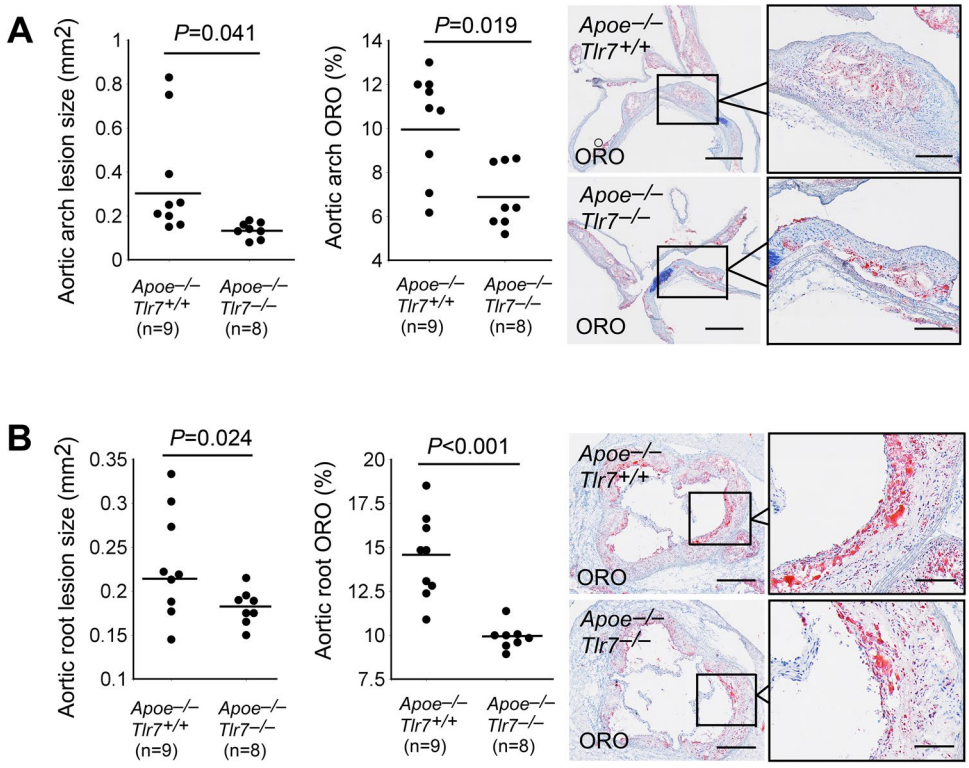

Figure 2. TLR7 deficiency reduces atherosclerotic lesion size and lesion lipid deposition in male *Apoe*$^{-/-}$ mice after 3 months of an atherogenic diet. (**A**) Aortic arch lesion size (left), ORO staining detected lipid deposition (middle), and aortic arch ORO staining representative images. Scale: 1 mm, inset scale: 200 μm. (**B**) Aortic root lesion size (left), ORO staining detected lipid deposition (middle), and aortic root ORO staining representative images. Scale: 1 mm, inset scale: 200 μm. Numbers (in parentheses) and genotypes of mice are indicated.

and adventitia in aortic arches from *Apoe*$^{-/-}$ mice that had consumed an atherogenic diet for 3 months (Fig. 1B). Immunostaining of a parallel section using a rabbit IgG isotype, as negative control, revealed negligible signal (Fig. 1C).

Immunofluorescent double staining of mouse aortic arch atherosclerotic lesions from *Apoe*$^{-/-}$ mice demonstrated TLR7 expression in macrophages (Fig. 1D, left two panels), SMCs (Fig. 1E, middle two panels), and ECs in both the lumen and adventitia microvessels (Fig. 1F, right three panels).

TLR7 deficiency reduced atherosclerosis and lesion inflammation. To test a direct role of TLR7 in atherosclerosis, we generated *Apoe*$^{-/-}$ *Tlr7*$^{-/-}$ and *Apoe*$^{-/-}$ *Tlr7*$^{+/+}$ littermate control mice. To induce atherosclerosis, we fed 8 to 10 weeks old male mice an atherogenic diet for 3 months. Mouse bodyweights or blood pressures did not differ between the two types of mice before or after the atherogenic diet. We assessed atherosclerotic lesion sizes in both the aortic arch and aortic root by staining frozen sections with ORO. In aortic arches, ORO staining revealed significantly smaller atherosclerotic lesions and lipid deposition areas from *Apoe*$^{-/-}$ *Tlr7*$^{-/-}$ mice than those from *Apoe*$^{-/-}$ *Tlr7*$^{+/+}$ control mice (Fig. 2A). We obtained similar conclusion when mouse aortic roots were analyzed. ORO staining also demonstrated significantly smaller atherosclerotic lesions and lipid deposition areas in aortic roots from *Apoe*$^{-/-}$ *Tlr7*$^{-/-}$ mice than those from *Apoe*$^{-/-}$ *Tlr7*$^{+/+}$ control mice (Fig. 2B).

We measured lesion contents of macrophages, CD4^{+} T cells, and MHC-II levels as indication of inflammatory cell infiltration and inflammation according to previously described methods[28]. Compared with the *Apoe*$^{-/-}$ *Tlr7*$^{+/+}$ control mice, aortic arches from *Apoe*$^{-/-}$ *Tlr7*$^{-/-}$ mice had significantly smaller Mac-3-positive macrophage areas (Fig. 3A), fewer lesion CD4^{+} T cells (Fig. 3B), and smaller MHC-II-positive areas (Fig. 3C). Significant smaller aortic arch atherosclerotic lesion sizes in *Apoe*$^{-/-}$ *Tlr7*$^{-/-}$ mice than those in *Apoe*$^{-/-}$ *Tlr7*$^{+/+}$ control mice may account for reduced lesion contents of macrophages, CD4^{+} T cells, and MHC-II-positive areas from *Apoe*$^{-/-}$ *Tlr7*$^{-/-}$ mice. When Mac-3-positive macrophage areas were expressed as percentage of total lesion areas, the macrophage contents in *Apoe*$^{-/-}$ *Tlr7*$^{+/+}$ control mice remained higher than those in *Apoe*$^{-/-}$ *Tlr7*$^{-/-}$ mice, but such a difference did not reach statistical significance ($26.27 \pm 11.34\%$ *vs.* $10.50 \pm 2.51\%$, $P = 0.141$) (Fig. 3D). Similarly, when CD4^{+} T-cell numbers were expressed as those of each mm^2, we found comparable lesion CD4^{+} T-cell contents between *Apoe*$^{-/-}$ *Tlr7*$^{+/+}$ control mice and *Apoe*$^{-/-}$ *Tlr7*$^{-/-}$ mice (14.90 ± 3.45 number/mm^2 *vs.* 18.10 ± 3.30 number/mm^2, $P = 0.341$) (Fig. 3E). However, when MHC-II-positive areas were expressed as percentage of total lesion areas, we still saw significantly higher lesion MHC-II contents in *Apoe*$^{-/-}$ *Tlr7*$^{+/+}$ control mice than in *Apoe*$^{-/-}$ *Tlr7*$^{-/-}$ mice ($42.13 \pm 10.11\%$ *vs.* $5.67 \pm 1.03\%$, $P = 0.002$) (Fig. 3F).

IL6 is an important TLR7 downstream inflammatory product. TLR7 activation increases IL6 production[33,34]. IFN-γ is another common pro-inflammatory cytokine in atherosclerosis. TLR7 activation can also indirectly

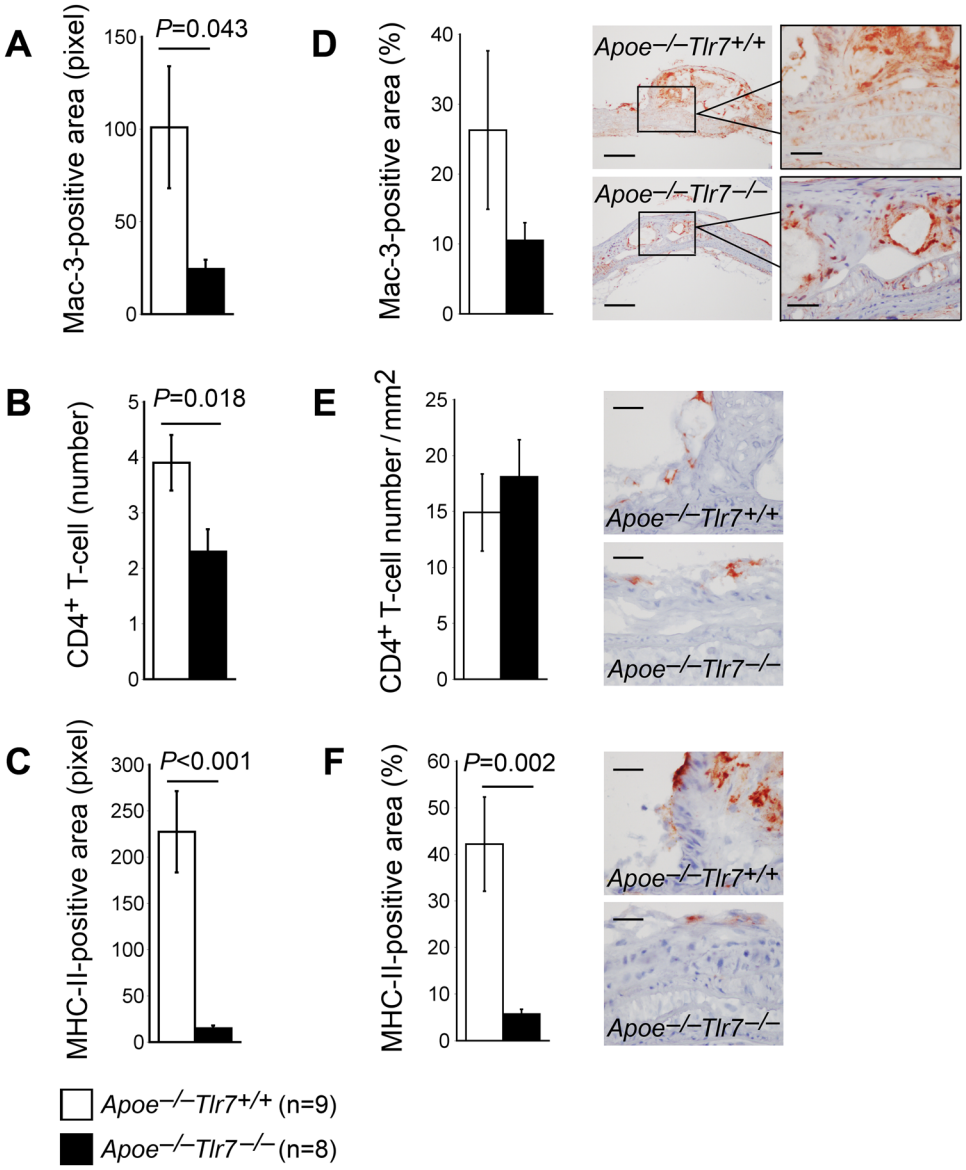

Figure 3. TLR7 deficiency and aortic arch atherosclerotic lesion inflammatory cell accumulation in male *Apoe*$^{-/-}$ mice. (**A**) Mac-3-positive area in pixel. (**B**) Lesion CD4^{+} T-cell number. (**C**) Lesion MHC class-II-positive area in pixel. (**D**) Mac-3-positive area versus total lesion area in percentage. Representative images are shown to the right. Scale: 200 μm, inset scale: 100 μm. (**E**) Lesion CD4^{+} T-cell number per mm^{2}. Representative images are shown to the right. Scale: 100 μm. (**F**) Lesion MHC class-II-positive area versus total lesion area in percentage. Representative images are shown to the right. Scale: 100 μm. Numbers and genotypes of mice are indicated in the legends.

produce IFN-γ[35,36]. In contrast, TLR7 activation decreases TGF-β expression[37]. In turn, TGF-β inhibits TLR7 downstream pro-inflammatory molecule expression[38,39]. IL4 is an anti-inflammatory cytokine that regulates TLR7 responses to viral infections[40] or B-cell activation[41]. Therefore, TLR7 deficiency may attenuate atherosclerosis (Fig. 2A and B) by altering the production of these pro- and anti-inflammatory cytokines. Mouse plasma IFN-γ levels were undetectable by ELISA. Plasma IL6 levels from *Apoe*$^{-/-}$ *Tlr7*$^{-/-}$ mice were lower than those from the *Apoe*$^{-/-}$ *Tlr7*$^{+/+}$ littermates, but such a difference did not reach statistical significance (Fig. 4A). In the aortic arches, however, lesion IL6-positive areas were significantly lower in *Apoe*$^{-/-}$ *Tlr7*$^{-/-}$ mice than those in *Apoe*$^{-/-}$ *Tlr7*$^{+/+}$ mice (Fig. 4B, left and middle panels). Rabbit anti-mouse IL6 antibody specificity in mouse aortic arch immunostaining was verified using rabbit IgG isotype to stain the parallel sections and showed no immunoreactive signals (Fig. 4B, right panels). Lesion anti-inflammatory cytokines IL4- and TGF-β-positive areas were slightly elevated in aortic arches from the *Apoe*$^{-/-}$ *Tlr7*$^{-/-}$ mice, but such changes were also not statistically significant, compared with those from the *Apoe*$^{-/-}$ *Tlr7*$^{+/+}$ littermate control mice (Fig. 4C,D). Consistent with the hypothesis that TLR7 deficiency reduces lesion or systemic inflammation, plasma inflammation marker SAA was found significantly lower in *Apoe*$^{-/-}$ *Tlr7*$^{-/-}$ mice than in *Apoe*$^{-/-}$ *Tlr7*$^{+/+}$ control mice (Fig. 4E).

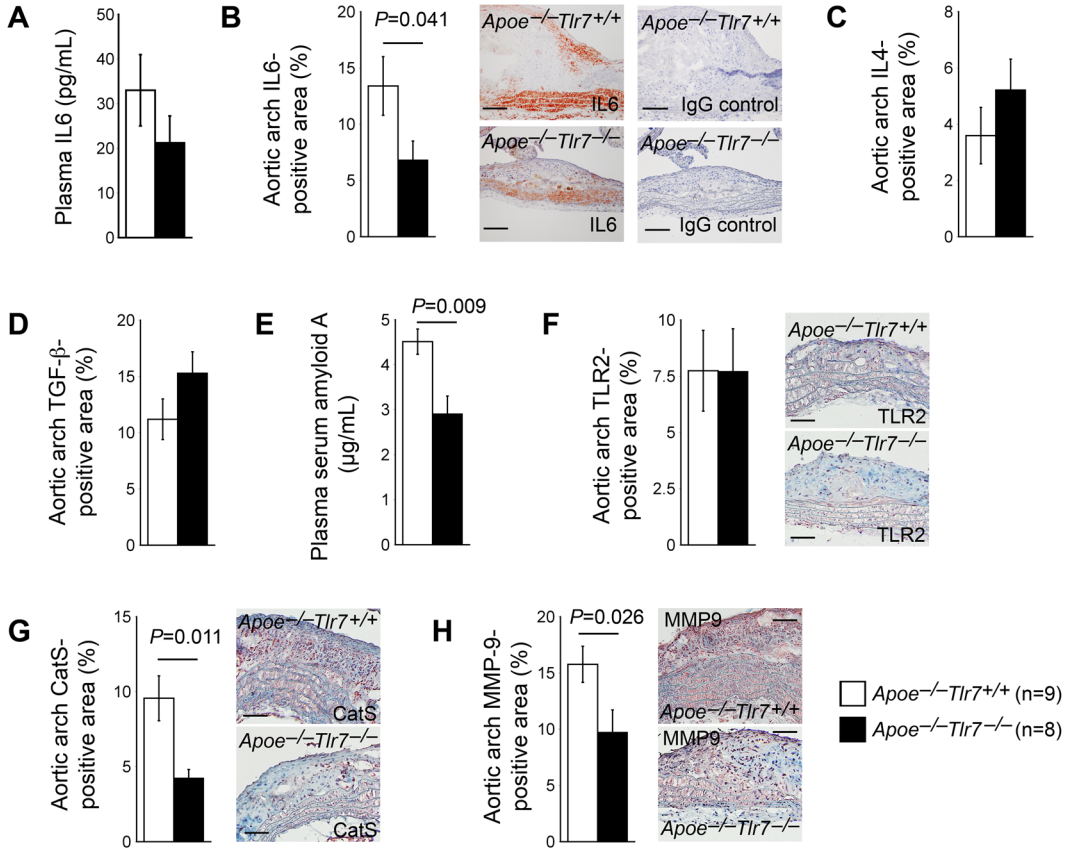

Figure 4. TLR7 deficiency changes aortic arch atherosclerotic lesion inflammatory cytokine and protease expression in male *Apoe*$^{-/-}$ mice. (**A**) Plasma IL6 level. (**B**) Lesion IL6-positive area percentage. Representative images are shown in the middle panels. Rabbit IgG isotype control staining results from parallel sections are show in the right panels. Scale: 200 μm. (**C**) Lesion IL4-positive area percentage. (**D**) Lesion TGF-β-positive area percentage. (**E**) Plasma SAA level. Lesion TLR2-positive area (**F**), CatS-positive area (**G**), and MMP-9-positive area (**H**) percentages. Representative images are shown to the right panels. Scales: 100 μm. Numbers and genotypes of mice are indicated in the legends.

Both endolysosomal TLRs (e.g. TLR7, and TLR9) and cell surface TLRs (e.g. TLR2 and TLR4) share the same MyD88 and IRAK4/TRAF6 signaling pathways that lead to the production of pro-inflammatory cytokines[22,42]. TLR7 deficiency is expected to reduce the production of lesion pro-inflammatory IL6 (Fig. 4B). Yet, it is also possible that endolysosomal TLR7 deficiency may affect the expression of cell surface TLRs. Therefore, reduced lesion IL6 (Fig. 4B) may come not only from TLR7 deficiency but also impaired expression of cell surface TLRs. We tested this possibility by immunostaining aortic arch atherosclerotic lesion TLR2 expression and did not detect significant differences in TLR2 expression in lesions between the *Apoe*$^{-/-}$ *Tlr7*$^{-/-}$ and *Apoe*$^{-/-}$ *Tlr7*$^{+/+}$ control mice (Fig. 4F). Instead, we found that atherosclerotic lesions from *Apoe*$^{-/-}$ *Tlr7*$^{-/-}$ mice contained significantly lower levels of both CatS (Fig. 4G) and MMP-9 (Fig. 4H), two common proteases that have been reported from atherosclerotic lesions, up-regulated by inflammatory cytokines, and play detrimental roles in atherogenesis[43–45].

TLR7 deficiency reduced lesion SMC loss and cell death. SMCs are the main cell type in the arterial wall and maintain the tissue phenotype and functional plasticity. These cells may switch their contractile phenotype into pro-inflammatory phenotype during atherogenesis-mediated inflammation, thereby undergoing apoptosis and cell loss[46]. SMC loss is associated with plaque rupture and lesion outward remodeling, and potential aneurysm formation[47,48]. Indeed, plaques from patients with atherosclerosis with unstable symptoms showed higher levels of apoptosis than those with stable lesions[49]. In aortic arches from *Apoe*$^{-/-}$ *Tlr7*$^{-/-}$ mice, we found significantly lower grade of SMC loss than that from *Apoe*$^{-/-}$ *Tlr7*$^{+/+}$ control mice (Fig. 5A). As expected, we detected significantly fewer TUNEL-positive apoptotic cells in the aortic arch media (Fig. 5B) and intima (Fig. 5C) from *Apoe*$^{-/-}$ *Tlr7*$^{-/-}$ mice than those from *Apoe*$^{-/-}$ *Tlr7*$^{+/+}$ mice. To determine the cell types that underwent apoptosis in atherosclerotic lesions from these mice, we performed immunofluorescent double staining using anti-mouse cleaved caspase-3 and antibodies against SMC α-smooth muscle actin and macrophage Mac-2. Cleaved caspase-3 and α-actin double positive apoptotic SMCs were detected in both the intima (Fig. 5D) and media (Fig. 5E) from *Apoe*$^{-/-}$ *Tlr7*$^{+/+}$ and *Apoe*$^{-/-}$ *Tlr7*$^{-/-}$ mice. We also detected cleaved caspase-3 and Mac-2 double positive apoptotic macrophages in atherosclerotic lesions from both *Apoe*$^{-/-}$ *Tlr7*$^{+/+}$ and *Apoe*$^{-/-}$ *Tlr7*$^{-/-}$ mice (Fig. 5F).

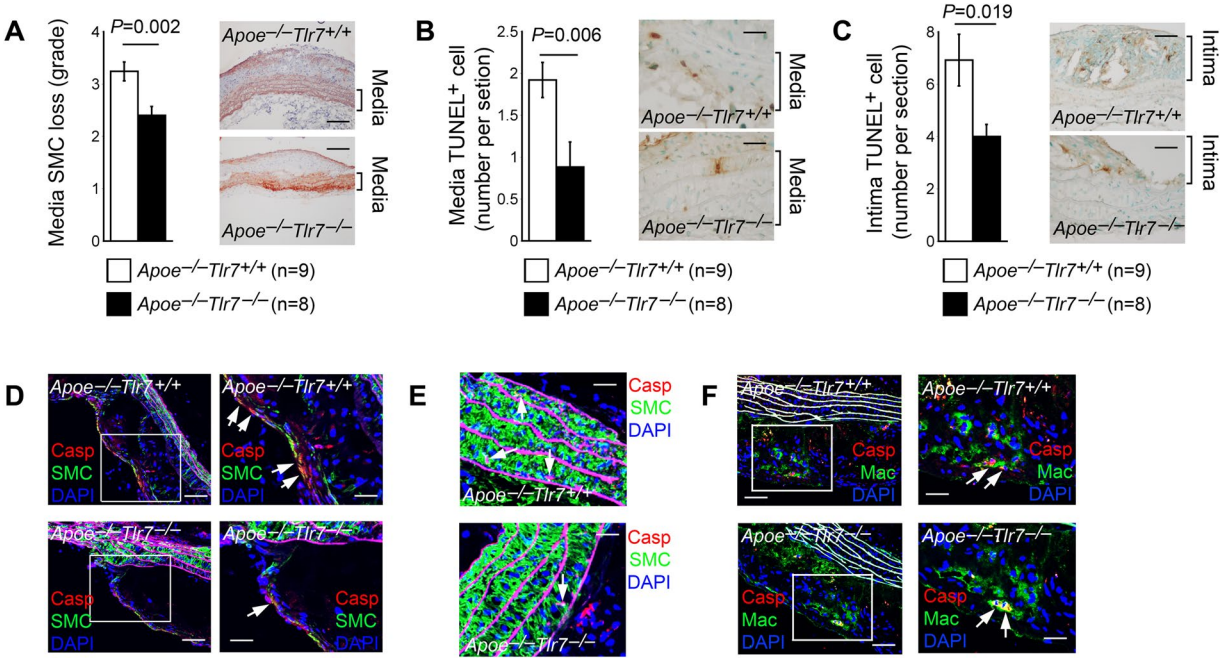

Figure 5. TLR7 deficiency reduces aortic arch atherosclerotic lesion SMC loss and cell apoptosis in male *Apoe*$^{-/-}$ mice. (**A**) Media SMC loss grade. Scale: 200 μm. (**B**) Media TUNEL-positive apoptotic cell number per section. Scale: 100 μm. (**C**) Intima TUNEL-positive apoptotic cell number per section. Scale: 100 μm. Media with clear elastic fibers and intima are framed. Representative images are shown to the middle panels. (**D**) Immunofluorescent double staining detected cleaved caspase-3 (Casp)-positive apoptotic SMC in the intima. Scale: 200 μm. Inset scale: 100 μm. (**E**) Cleaved caspase-3 (Casp)-positive apoptotic SMC in the media. Scale: 100 μm. (**F**) Cleaved caspase-3 (Casp)-positive apoptotic macrophages (Mac) in the lesions. Scale: 200 μm. Inset scale: 100 μm. Arrows indicate apoptotic cells. Numbers and genotypes of mice are indicated in the legends.

TLR7 deficiency did not affect arterial wall matrix protein expression or plasma lipoproteins. Besides apoptosis, media SMC loss may also be associated with elastin degradation[50]. Collagen is also a major component of the fibrotic cap that maintains the cap strength and integrity[51]. While CatS is a potent elastase[52], MMP-9 has both elastinolytic and collagenolytic activities[53–55]. Reduced expression of lesion CatS and MMP-9 in *Apoe*$^{-/-}$ *Tlr7*$^{-/-}$ mice may reduce lesion elastin fragmentation and increase collagen deposition. Yet, both elastin fragmentation and collagen contents in the aortic arches from both *Apoe*$^{-/-}$ *Tlr7*$^{-/-}$ and *Apoe*$^{-/-}$ *Tlr7*$^{+/+}$ mice did not differ (Fig. 6A,B), suggesting that the reduced media SMC loss in *Apoe*$^{-/-}$ *Tlr7*$^{-/-}$ mice was not due to changes in arterial wall elastin and collagen contents, although expression of both CatS and MMP-9 was reduced in lesions from these mice. Reduced lesion expression of these proteases in *Apoe*$^{-/-}$ *Tlr7*$^{-/-}$ mice may contribute to reduced lesion cell apoptosis as both are known to promote cell apoptosis[56,57]. Elevated plasma total cholesterol, LDL, and triglyceride levels, and reduced plasma HDL are associated with the development of atherosclerosis in humans and mice[58,59]. After consuming an atherogenic diet for 3 months, both *Apoe*$^{-/-}$ *Tlr7*$^{-/-}$ and *Apoe*$^{-/-}$ *Tlr7*$^{+/+}$ mice had comparable levels of plasma total cholesterol, LDL, triglyceride, and HDL (Fig. 6C–F).

Discussion

TLR7 is an endolysosome membrane receptor that mediates endogenous antigen or viral/bacterial ssRNA-induced inflammation[14,15,60]. This study demonstrated a detrimental role of TLR7 in diet-induced atherosclerosis in *Apoe*$^{-/-}$ mice by increasing lesion inflammation (MHC-II), lesion pro-inflammatory cytokine expression (IL6), lesion protease expression (CatS, and MMP-9), and systemic inflammation (plasma SAA). However, our observations are controversial to what were reported in *Apoe*$^{-/-}$ mice that consumed a chow diet[21], although this current study agrees with the observations that TLR7 antagonist blocked macrophage activation, foam cell formation, and neointima development in a femoral artery cuff placement-induced neointima thickening in ApoE*3-Leiden mice[23]. Our study also agrees with the conclusion from the hypercholesterolemic rabbits, in which TLR7 activation with imiquimod increased collar placement-induced carotid artery atherosclerotic lesion intima area, lipid deposition, proteoglycan level, macrophage contents, T cell contents, and angiogenesis[24].

In male *Apoe*$^{-/-}$ mouse spontaneous atherosclerosis from the study by Salagianni *et al.*[21], atherosclerotic lesion in the aortic root was enlarged in the absence of TLR7, along with elevated lesion lipid and macrophage contents, compared with the *Apoe*$^{-/-}$ control mice. In our study, after feeding the same male *Apoe*$^{-/-}$ *Tlr7*$^{-/-}$ mice an atherogenic diet, we detected reduced atherosclerosis and lipid deposition in both aortic arch and root from these mice, compared with the *Apoe*$^{-/-}$*Tlr7*$^{+/+}$ littermates. It is possible that such discrepancies between the two studies were because of the differences in diet components. Dietary and commensal sources of PAMPs may activate TLR7 differently between chow and high cholesterol diets[61]. Indeed, similar atherosclerosis phenotype

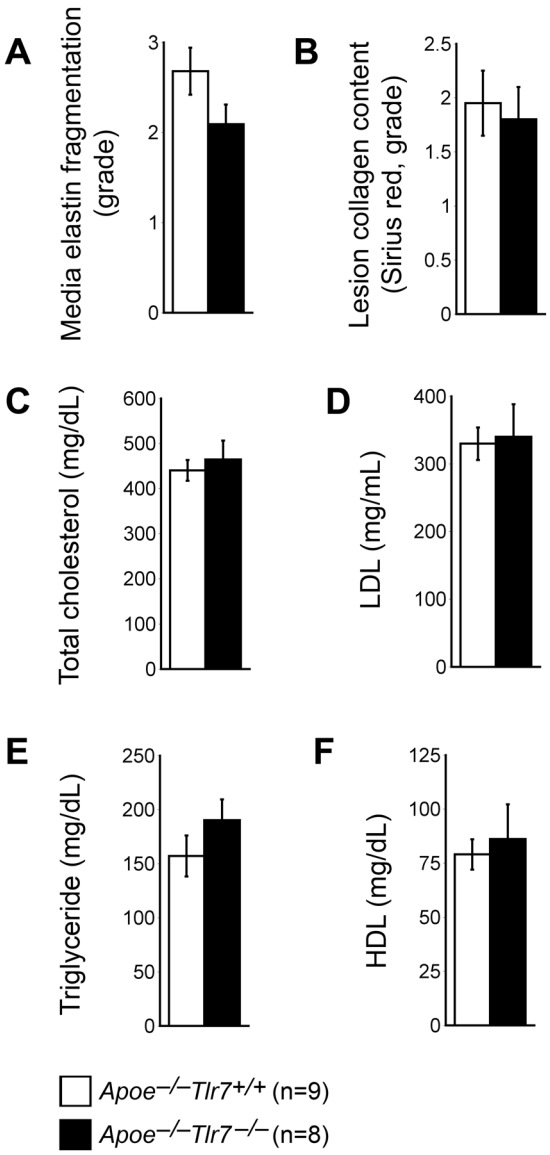

Figure 6. TLR7 deficiency does not affect aortic arch lesion matrix proteins or plasma lipid profile. (**A**) Lesion elastin fragmentation grade. (**B**) Lesion Sirius red-positive collagen grade. (**C–F**) Plasma total cholesterol, LDL, triglyceride, and HDL levels. Numbers and genotypes of mice are indicated in the legends.

changes because of diet differences (chow diet *versus* atherogenic diet) have been reported previously in the same male IL18-deficient *Apoe*$^{-/-}$ (*Apoe*$^{-/-}$*Il18*$^{-/-}$) mice. When mice were fed a chow diet and analyzed at 24 weeks of age, spontaneous atherosclerotic lesions were significantly reduced in *Apoe*$^{-/-}$*Il18*$^{-/-}$ mice, compared with those in *Apoe*$^{-/-}$ control mice[62]. In contrast, when the same mice were fed a high cholesterol atherogenic diet at 5 weeks of age for 12 weeks, *Apoe*$^{-/-}$*Il18*$^{-/-}$ mice developed significantly larger atherosclerotic lesions than did the *Apoe*$^{-/-}$ mice[63]. It was hypothesized that atherogenic diet may alter local and systemic inflammation[63]. The role of endolysosomal TLR in atherosclerosis has been controversial among all tested members. In atherogenic diet-fed *Ldlr*$^{-/-}$ and *Apoe*$^{-/-}$ mice, genetic depletion of TLR3 protected the mouse aortic wall from medial degradation with increased lesion collagen deposition and medial SMC content, although TLR3 deficiency did not affect lesion areas[7]. In contrast, when *Apoe*$^{-/-}$ mice were fed a chow diet for 15 weeks, TLR3 deficiency increased aortic lesion atherosclerotic lesion area[12]. A major difference between the two studies is the diet. However, diet alone may not explain the discrepancies between these studies. In *Apoe*$^{-/-}$ mice on a chow diet, TLR9 antagonist reduced aortic root atherosclerosis with decreased lesion inflammatory cell accumulation and increased lesion collagen and SMCs[64]. In ApoE*3 Leiden mice being fed a chow diet, TLR9 antagonist also reduced femoral artery cuff placement-induced neointima thickening and foam cell formation[23]. When *Apoe*$^{-/-}$ mice were on an atherogenic diet for 7 weeks, TLR9 activation with a high dose of its agonist CpG oligodeoxynucleotide (ODN)1826 enhanced atherosclerosis in the aortic root[65]. All these observations, regardless of diet types, point to a detrimental role of TLR9 in atherosclerosis. However, in an independent study of *Apoe*$^{-/-}$ mice on an atherogenic diet for 8 weeks, TLR9 deficiency (*Apoe*$^{-/-}$ *Tlr9*$^{-/-}$) increased aortic root atherosclerosis and lesion CD4^{+} T-cell content.

$CD4^+$ T-cell depletion in these mice reduced atherosclerosis, suggesting a role of TLR9 in regulating $CD4^+$ T cells in atherosclerosis. In the same study, TLR9 activation with its agonist CpG ODN1668 decreased aortic root atherosclerosis[13]. These observations suggest a protective role of TLR9 in atherosclerosis. Obviously, the use of different diets may not explain all the discrepancies in the role of TLR9 in atherosclerosis and additional mechanisms may be involved and merit further investigation. A high cholesterol atherogenic diet is commonly used to produce atherosclerosis in atherosclerosis-prone *Apoe*$^{-/-}$ mice or in *Ldlr*$^{-/-}$mice[66–69]. Such diet may lead to steatosis and systemic inflammation, as part of its mechanism in atherosclerosis, abdominal aortic aneurysm, obesity, and diabetes studies[66–72]. Reduced atherosclerotic lesion IL6 expression and plasma SAA levels in *Apoe*$^{-/-}$ *Tlr7*$^{-/-}$ mice compared with those from *Apoe*$^{-/-}$ control mice from our study supported a role of TLR7 in regulating local and systemic inflammation. An atherogenic diet may affect TLR7 activation cascade, thereby changing downstream inflammatory molecule expression and atherogenesis. This hypothesis is consistent to several prior studies. For example, in C57BL/6 wild-type mice, TLR7 activation with R848 induced the production of IL10, IL6, TNF-α, and IL12 in a dose- and time-dependent manner[73]. In mouse macrophages, TLR7 activation with imiquimod induced macrophage production of IL6, MCP-1, RANTES (regulated on activation, normal T cell expressed and secreted), and TNF-α[24]. Effector T cells from imiquimod-treated squamous cell carcinomas produced more IFN-γ, granzyme, and perforin, and less IL-10 and TGF-β than T cells from untreated tumors[74]. All these data indicate a pro-inflammatory role of TLR7 in macrophages and lymphocytes. However, we cannot explain why macrophages from *Tlr7*$^{-/-}$ mice responded to TLR2 ligand lipoteichoic acid and produced significantly more MCP-1, IL6, and IL10 than those from wild-type control mice in a study from Salagianni *et al.*[21].

Different from endolysosomal TLRs, cell surface TLRs such as TLR2 and TLR4 have been proven detrimental in atherosclerosis from most tested experimental models. In *Apoe*$^{-/-}$ mice on an atherogenic diet or a chow diet, deficiency of TLR4 or its signaling molecule MyD88 reduced aortic atherosclerosis, lesion lipid and macrophage contents, and peripheral IL1α, IL2 and MCP-1 levels[75,76]. Similar observations were made in *Ldlr*$^{-/-}$ mice. Deficiency of TLR4 reduced atherosclerosis and plasma cholesterol and triglyceride, although did not affect obesity, hyperinsulinemia, or glucose intolerance after mice were fed a diabetogenic diet[8]. Similarly, TLR2-deficient *Apoe*$^{-/-}$ mice on a chow diet or an atherogenic diet or *Apoe*$^{-/-}$ mice on a chow diet but treated with an anti-mouse TLR2 antibody all demonstrated reduced atherosclerotic lesion size, lipid accumulation, macrophage and MCP-1 contents, and expression of cytokines (TNF-α and IL6) and associated transcription factors (NF-κB and STAT3)[77,78]. It is possible that dietary and commensal sources of PAMPs from mice fed a chow and a high cholesterol diets may activate endolysosomal TLRs differently from cell surface TLRs[61], a hypothesis that was not tested in this study.

The exact ligands that activate TLR7 during atherogenesis remain unknown. This is an interesting and important topic for further exploration. Endogenous TLR7 ligands include mainly ssRNA such as those from viral infections[79–81], or even single nucleotide such as guanosine (G)/2′-deoxyguanosine (dG)[82]. Such nucleotide(s) in atherosclerotic lesions may activate TLR7 and promote atherosclerosis. For example, hepatitis C virus RNA and active cytomegalovirus were found in human atherosclerotic lesions[83,84]. Hepatitis C infection facilitates human atherosclerosis[85] and herpesvirus infection accelerates atherosclerosis in the *Apoe*$^{-/-}$ mice[86]. It is possible that these virus affects atherosclerosis by activating TLR7. Nevertheless, results from this study support a pro-inflammatory role of TLR7 in atherogenic diet-induced atherosclerosis in *Apoe*$^{-/-}$ mice. It is possible that TLR7 antagonists may have therapeutic potential in atherosclerosis and possibly other cardiovascular diseases[87].

References

1. Akira, S., Uematsu, S. & Takeuchi, O. Pathogen recognition and innate immunity. *Cell* **124**, 783–801, doi:10.1016/j.cell.2006.02.015 (2006).
2. Thompson, M. R., Kaminski, J. J., Kurt-Jones, E. A. & Fitzgerald, K. A. Pattern recognition receptors and the innate immune response to viral infection. *Viruses* **3**, 920–940, doi:10.3390/v3060920 (2011).
3. Hovland, A. *et al.* The complement system and toll-like receptors as integrated players in the pathophysiology of atherosclerosis. *Atherosclerosis* **241**, 480–494, doi:10.1016/j.atherosclerosis.2015.05.038 (2015).
4. Elsenberg, E. H. *et al.* Increased cytokine response after toll-like receptor stimulation in patients with stable coronary artery disease. *Atherosclerosis* **231**, 346–351, doi:10.1016/j.atherosclerosis.2013.09.036 (2013).
5. Cole, J. E., Kassiteridi, C. & Monaco, C. Toll-like receptors in atherosclerosis: a 'Pandora's box' of advances and controversies. *Trends Pharmacol Sci* **34**, 629–636, doi:10.1016/j.tips.2013.09.008 (2013).
6. Lundberg, A. M. *et al.* Toll-like receptor 3 and 4 signalling through the TRIF and TRAM adaptors in haematopoietic cells promotes atherosclerosis. *Cardiovasc Res* **99**, 364–373, doi:10.1093/cvr/cvt033 (2013).
7. Ishibashi, M., Sayers, S., D'Armiento, J. M., Tall, A. R. & Welch, C. L. TLR3 deficiency protects against collagen degradation and medial destruction in murine atherosclerotic plaques. *Atherosclerosis* **229**, 52–61, doi:10.1016/j.atherosclerosis.2013.03.035 (2013).
8. Ding, Y. *et al.* Toll-like receptor 4 deficiency decreases atherosclerosis but does not protect against inflammation in obese low-density lipoprotein receptor-deficient mice. *Arterioscler Thromb Vasc Biol* **32**, 1596–1604, doi:10.1161/ATVBAHA.112.249847 (2012).
9. Hasu, M., Thabet, M., Tam, N. & Whitman, S. C. Specific loss of toll-like receptor 2 on bone marrow derived cells decreases atherosclerosis in LDL receptor null mice. *Can J Physiol Pharmacol* **89**, 737–742, doi:10.1139/y11-071 (2011).
10. Lu, Z., Zhang, X., Li, Y., Jin, J. & Huang, Y. TLR4 antagonist reduces early-stage atherosclerosis in diabetic apolipoprotein E-deficient mice. *J Endocrinol* **216**, 61–71, doi:10.1530/JOE-12-0338 (2013).
11. Hayashi, C. *et al.* Protective role for TLR4 signaling in atherosclerosis progression as revealed by infection with a common oral pathogen. *J Immunol* **189**, 3681–3688, doi:10.4049/jimmunol.1201541 (2012).
12. Cole, J. E. *et al.* Unexpected protective role for Toll-like receptor 3 in the arterial wall. *Proc Natl Acad Sci USA* **108**, 2372–2377, doi:10.1073/pnas.1018515108 (2011).
13. Koulis, C. *et al.* Protective role for Toll-like receptor-9 in the development of atherosclerosis in apolipoprotein E-deficient mice. *Arterioscler Thromb Vasc Biol* **34**, 516–525, doi:10.1161/ATVBAHA.113.302407 (2014).
14. Lund, J. M. *et al.* Recognition of single-stranded RNA viruses by Toll-like receptor 7. *Proc Natl Acad Sci USA* **101**, 5598–5603, doi:10.1073/pnas.0400937101 (2004).
15. Lau, C. M. *et al.* RNA-associated autoantigens activate B cells by combined B cell antigen receptor/Toll-like receptor 7 engagement. *J Exp Med* **202**, 1171–1177, doi:10.1084/jem.20050630 (2005).

16. Hackl, D., Loschko, J., Sparwasser, T., Reindl, W. & Krug, A. B. Activation of dendritic cells via TLR7 reduces Foxp3 expression and suppressive function in induced Tregs. *Eur J Immunol* **41**, 1334–1343, doi:10.1002/eji.201041014 (2011).
17. Pasare, C. & Medzhitov, R. Toll pathway-dependent blockade of CD4 + CD25 + T cell-mediated suppression by dendritic cells. *Science* **299**, 1033–1036, doi:10.1126/science.1078231 (2003).
18. Meng, X. *et al*. Regulatory T cells prevent plaque disruption in apolipoprotein E-knockout mice. *Int J Cardiol* **168**, 2684–2692, doi:10.1016/j.ijcard.2013.03.026 (2013).
19. Klingenberg, R. *et al*. Depletion of FOXP3 + regulatory T cells promotes hypercholesterolemia and atherosclerosis. *J Clin Invest* **123**, 1323–1334, doi:10.1172/JCI63891 (2013).
20. Pryshchep, O., Ma-Krupa, W., Younge, B. R., Goronzy, J. J. & Weyand, C. M. Vessel-specific Toll-like receptor profiles in human medium and large arteries. *Circulation* **118**, 1276–1284, doi:10.1161/CIRCULATIONAHA.108.789172 (2008).
21. Salagianni, M. *et al*. Toll-like receptor 7 protects from atherosclerosis by constraining "inflammatory" macrophage activation. *Circulation* **126**, 952–962, doi:10.1161/CIRCULATIONAHA.111.067678 (2012).
22. Kawai, T. & Akira, S. The role of pattern-recognition receptors in innate immunity: update on Toll-like receptors. *Nat Immunol* **11**, 373–384, doi:10.1038/ni.1863 (2010).
23. Karper, J. C. *et al*. Blocking toll-like receptors 7 and 9 reduces postinterventional remodeling via reduced macrophage activation, foam cell formation, and migration. *Arterioscler Thromb Vasc Biol* **32**, e72–80, doi:10.1161/ATVBAHA.112.249391 (2012).
24. De Meyer, I. *et al*. Toll-like receptor 7 stimulation by imiquimod induces macrophage autophagy and inflammation in atherosclerotic plaques. *Basic Res Cardiol* **107**, 269, doi:10.1007/s00395-012-0269-1 (2012).
25. Erridge, C. *et al*. Vascular cell responsiveness to Toll-like receptor ligands in carotid atheroma. *Eur J Clin Invest* **38**, 713–720, doi:10.1111/j.1365-2362.2008.02010.x (2008).
26. Watkins, A. A. *et al*. IRF5 deficiency ameliorates lupus but promotes atherosclerosis and metabolic dysfunction in a mouse model of lupus-associated atherosclerosis. *J Immunol* **194**, 1467–1479, doi:10.4049/jimmunol.1402807 (2015).
27. Venegas-Pino, D. E., Banko, N., Khan, M. I., Shi, Y. & Werstuck, G. H. Quantitative analysis and characterization of atherosclerotic lesions in the murine aortic sinus. *J Vis Exp*, 50933, 10.3791/50933 (2013).
28. Mach, F., Schonbeck, U., Sukhova, G. K., Atkinson, E. & Libby, P. Reduction of atherosclerosis in mice by inhibition of CD40 signalling. *Nature* **394**, 200–203, doi:10.1038/28204 (1998).
29. Shi, G. P. *et al*. Human cathepsin S: chromosomal localization, gene structure, and tissue distribution. *J Biol Chem* **269**, 11530–11536 (1994).
30. Kitamoto, S. *et al*. Cathepsin L deficiency reduces diet-induced atherosclerosis in low-density lipoprotein receptor-knockout mice. *Circulation* **115**, 2065–2075, doi:10.1161/CIRCULATIONAHA.107.688523 (2007).
31. Sun, J. *et al*. Mast cells modulate the pathogenesis of elastase-induced abdominal aortic aneurysms in mice. *J Clin Invest* **117**, 3359–3368, doi:10.1172/JCI31311 (2007).
32. Friedewald, W. T., Levy, R. I. & Fredrickson, D. S. Estimation of the concentration of low-density lipoprotein cholesterol in plasma, without use of the preparative ultracentrifuge. *Clin Chem* **18**, 499–502 (1972).
33. Bush, T. J. & Bishop, G. A. TLR7 and CD40 cooperate in IL-6 production via enhanced JNK and AP-1 activation. *Eur J Immunol* **38**, 400–409, doi:10.1002/(ISSN)1521-4141 (2008). anden.
34. Li, L. *et al*. The activation of TLR7 regulates the expression of VEGF, TIMP1, MMP2, IL-6, and IL-15 in Hela cells. *Mol Cell Biochem* **389**, 43–49, doi:10.1007/s11010-013-1925-y (2014).
35. Girart, M. V., Fuertes, M. B., Domaica, C. I., Rossi, L. E. & Zwirner, N. W. Engagement of TLR3, TLR7, and NKG2D regulate IFN-gamma secretion but not NKG2D-mediated cytotoxicity by human NK cells stimulated with suboptimal doses of IL-12. *J Immunol* **179**, 3472–3479, doi:10.4049/jimmunol.179.6.3472 (2007).
36. Adib-Conquy, M., Scott-Algara, D., Cavaillon, J. M. & Souza-Fonseca-Guimaraes, F. TLR-mediated activation of NK cells and their role in bacterial/viral immune responses in mammals. *Immunol Cell Biol* **92**, 256–262, doi:10.1038/icb.2013.99 (2014).
37. Chen, J., Zeng, B., Yao, H. & Xu, J. The effect of TLR4/7 on the TGF-beta-induced Smad signal transduction pathway in human keloid. *Burns* **39**, 465–472, doi:10.1016/j.burns.2012.07.019 (2013).
38. Bekeredjian-Ding, I. *et al*. Tumour-derived prostaglandin E and transforming growth factor-beta synergize to inhibit plasmacytoid dendritic cell-derived interferon-alpha. *Immunology* **128**, 439–450, doi:10.1111/j.1365-2567.2009.03134.x (2009).
39. Saas, P. & Perruche, S. Functions of TGF-beta-exposed plasmacytoid dendritic cells. *Crit Rev Immunol* **32**, 529–553, doi:10.1615/CritRevImmunol.v32.i6 (2012).
40. Sriram, U. *et al*. IL-4 suppresses the responses to TLR7 and TLR9 stimulation and increases the permissiveness to retroviral infection of murine conventional dendritic cells. *PLoS One* **9**, e87668, doi:10.1371/journal.pone.0087668 (2014).
41. Tsukamoto, Y. *et al*. Toll-like receptor 7 cooperates with IL-4 in activated B cells through antigen receptor or CD38 and induces class switch recombination and IgG1 production. *Mol Immunol* **46**, 1278–1288, doi:10.1016/j.molimm.2008.11.022 (2009).
42. Kawasaki, T. & Kawai, T. Toll-like receptor signaling pathways. *Front Immunol* **5**, 461, doi:10.3389/fimmu.2014.00461 (2014).
43. Sukhova, G. K. *et al*. Deficiency of cathepsin S reduces atherosclerosis in LDL receptor-deficient mice. *J Clin Invest* **111**, 897–906, doi:10.1172/JCI200314915 (2003).
44. Luttun, A. *et al*. Loss of matrix metalloproteinase-9 or matrix metalloproteinase-12 protects apolipoprotein E-deficient mice against atherosclerotic media destruction but differentially affects plaque growth. *Circulation* **109**, 1408–1414, doi:10.1161/01.CIR.0000121728.14930.DE (2004).
45. Gough, P. J., Gomez, I. G., Wille, P. T. & Raines, E. W. Macrophage expression of active MMP-9 induces acute plaque disruption in apoE-deficient mice. *J Clin Invest* **116**, 59–69, doi:10.1172/JCI25074 (2006).
46. Chistiakov, D. A., Orekhov, A. N. & Bobryshev, Y. V. Vascular smooth muscle cell in atherosclerosis. *Acta Physiol (Oxf)* **214**, 33–50, doi:10.1111/apha.2015.214.issue-1 (2015).
47. Glagov, S., Weisenberg, E., Zarins, C. K., Stankunavicius, R. & Kolettis, G. J. Compensatory enlargement of human atherosclerotic coronary arteries. *N Engl J Med* **316**, 1371–1375, doi:10.1056/NEJM198705283162204 (1987).
48. Lopez-Candales, A. *et al*. Decreased vascular smooth muscle cell density in medial degeneration of human abdominal aortic aneurysms. *Am J Pathol* **150**, 993–1007 (1997).
49. Geng, Y. J. & Libby, P. Evidence for apoptosis in advanced human atheroma. *Colocalization with interleukin-1 beta-converting enzyme. Am J Pathol* **147**, 251–266 (1995).
50. Pai, A., Leaf, E. M., El-Abbadi, M. & Giachelli, C. M. Elastin degradation and vascular smooth muscle cell phenotype change precede cell loss and arterial medial calcification in a uremic mouse model of chronic kidney disease. *Am J Pathol* **178**, 764–773, doi:10.1016/j.ajpath.2010.10.006 (2011).
51. Adiguzel, E., Ahmad, P. J., Franco, C. & Bendeck, M. P. Collagens in the progression and complications of atherosclerosis. *Vasc Med* **14**, 73–89, doi:10.1177/1358863X08094801 (2009).
52. Chapman, H. A., Riese, R. J. & Shi, G. P. Emerging roles for cysteine proteases in human biology. *Annu Rev Physiol* **59**, 63–88, doi:10.1146/annurev.physiol.59.1.63 (1997).
53. Barascuk, N. *et al*. Development and validation of an enzyme-linked immunosorbent assay for the quantification of a specific MMP-9 mediated degradation fragment of type III collagen—A novel biomarker of atherosclerotic plaque remodeling. *Clin Biochem* **44**, 900–906, doi:10.1016/j.clinbiochem.2011.04.004 (2011).
54. Vassiliadis, E. *et al*. Measurement of matrix metalloproteinase 9-mediated collagen type III degradation fragment as a marker of skin fibrosis. *BMC Dermatol* **11**, 6, doi:10.1186/1471-5945-11-6 (2011).

55. Van Doren, S. R. Matrix metalloproteinase interactions with collagen and elastin. *Matrix Biol* **44-46**, 224–231, doi:10.1016/j.matbio.2015.01.005 (2015).
56. Zheng, T. *et al*. Role of cathepsin S-dependent epithelial cell apoptosis in IFN-gamma-induced alveolar remodeling and pulmonary emphysema. *J Immunol* **174**, 8106–8115, doi:10.4049/jimmunol.174.12.8106 (2005).
57. Newby, A. C. Matrix metalloproteinases regulate migration, proliferation, and death of vascular smooth muscle cells by degrading matrix and non-matrix substrates. *Cardiovasc Res* **69**, 614–624, doi:10.1016/j.cardiores.2005.08.002 (2006).
58. Upadhyay, R. K. Emerging risk biomarkers in cardiovascular diseases and disorders. *J Lipids* **2015**, 971453–50, doi:10.1155/2015/971453 (2015).
59. Chapman, M. J. *et al*. Triglyceride-rich lipoproteins and high-density lipoprotein cholesterol in patients at high risk of cardiovascular disease: evidence and guidance for management. *Eur Heart J* **32**, 1345–1361, doi:10.1093/eurheartj/ehr112 (2011).
60. Mancuso, G. *et al*. Bacterial recognition by TLR7 in the lysosomes of conventional dendritic cells. *Nat Immunol* **10**, 587–594, doi:10.1038/ni.1733 (2009).
61. Erridge, C. Diet, commensals and the intestine as sources of pathogen-associated molecular patterns in atherosclerosis, type 2 diabetes and non-alcoholic fatty liver disease. *Atherosclerosis* **216**, 1–6, doi:10.1016/j.atherosclerosis.2011.02.043 (2011).
62. Elhage, R. *et al*. Reduced atherosclerosis in interleukin-18 deficient apolipoprotein E-knockout mice. *Cardiovasc Res* **59**, 234–240, doi:10.1016/S0008-6363(03)00343-2 (2003).
63. Pejnovic, N. *et al*. Increased atherosclerotic lesions and Th17 in interleukin-18 deficient apolipoprotein E-knockout mice fed high-fat diet. *Mol Immunol* **47**, 37–45, doi:10.1016/j.molimm.2008.12.032 (2009).
64. Ma, C. *et al*. Toll-Like Receptor 9 Inactivation Alleviated Atherosclerotic Progression and Inhibited Macrophage Polarized to M1 Phenotype in ApoE$^{-/-}$Mice. *Dis Markers* **2015**, 909572, doi:10.1155/2015/909572 (2015).
65. Krogmann, A. O. *et al*. Proinflammatory Stimulation of Toll-Like Receptor 9 with High Dose CpG ODN 1826 Impairs Endothelial Regeneration and Promotes Atherosclerosis in Mice. *PLoS One* **11**, e0146326, doi:10.1371/journal.pone.0146326 (2016).
66. Ishibashi, S., Goldstein, J. L., Brown, M. S., Herz, J. & Burns, D. K. Massive xanthomatosis and atherosclerosis in cholesterol-fed low density lipoprotein receptor-negative mice. *J Clin Invest* **93**, 1885–1893, doi:10.1172/JCI117179 (1994).
67. Lichtman, A. H. *et al*. Hyperlipidemia and atherosclerotic lesion development in LDL receptor-deficient mice fed defined semipurified diets with and without cholate. *Arterioscler Thromb Vasc Biol* **19**, 1938–1944, doi:10.1161/01.ATV.19.8.1938 (1999).
68. Iwai, M. *et al*. Deletion of angiotensin II type 2 receptor exaggerated atherosclerosis in apolipoprotein E-null mice. *Circulation* **112**, 1636–1643, doi:10.1161/CIRCULATIONAHA.104.525550 (2005).
69. Chatterjee, S. *et al*. Inhibition of glycosphingolipid synthesis ameliorates atherosclerosis and arterial stiffness in apolipoprotein E$^{-/-}$ mice and rabbits fed a high-fat and -cholesterol diet. *Circulation* **129**, 2403–2413, doi:10.1161/CIRCULATIONAHA.113.007559 (2014).
70. Yang, M. *et al*. Cathepsin L activity controls adipogenesis and glucose tolerance. *Nat Cell Biol* **9**, 970–977, doi:10.1038/ncb1623 (2007).
71. Liu, J. *et al*. Genetic deficiency and pharmacological stabilization of mast cells reduce diet-induced obesity and diabetes in mice. *Nat Med* **15**, 940–945, doi:10.1038/nm.1994 (2009).
72. Liu, C. L. *et al*. Allergic Lung Inflammation Aggravates Angiotensin II-Induced Abdominal Aortic Aneurysms in Mice. *Arterioscler Thromb Vasc Biol* **36**, 69–77, doi:10.1161/ATVBAHA.115.305911 (2016).
73. Baenziger, S. *et al*. Triggering TLR7 in mice induces immune activation and lymphoid system disruption, resembling HIV-mediated pathology. *Blood* **113**, 377–388, doi:10.1182/blood-2008-04-151712 (2009).
74. Huang, S. J. *et al*. Imiquimod enhances IFN-gamma production and effector function of T cells infiltrating human squamous cell carcinomas of the skin. *J Invest Dermatol* **129**, 2676–2685, doi:10.1038/jid.2009.151 (2009).
75. Michelsen, K. S. *et al*. Lack of Toll-like receptor 4 or myeloid differentiation factor 88 reduces atherosclerosis and alters plaque phenotype in mice deficient in apolipoprotein E. *Proc Natl Acad Sci USA* **101**, 10679–10684, doi:10.1073/pnas.0403249101 (2004).
76. Higashimori, M. *et al*. Role of toll-like receptor 4 in intimal foam cell accumulation in apolipoprotein E-deficient mice. *Arterioscler Thromb Vasc Biol* **31**, 50–57, doi:10.1161/ATVBAHA.110.210971 (2011).
77. Liu, X. *et al*. Toll-like receptor 2 plays a critical role in the progression of atherosclerosis that is independent of dietary lipids. *Atherosclerosis* **196**, 146–154, doi:10.1016/j.atherosclerosis.2007.03.025 (2008).
78. Wang, X. X. *et al*. Blocking TLR2 activity diminishes and stabilizes advanced atherosclerotic lesions in apolipoprotein E-deficient mice. *Acta Pharmacol Sin* **34**, 1025–1035, doi:10.1038/aps.2013.75 (2013).
79. Jeffs, L. S., Nitschke, J., Tervaert, J. W., Peh, C. A. & Hurtado, P. R. Viral RNA in the influenza vaccine may have contributed to the development of ANCA-associated vasculitis in a patient following immunisation. *Clin Rheumatol* **35**, 943–951, doi:10.1007/s10067-015-3073-0 (2016).
80. Yu, X. *et al*. Toll-like receptor 7 promotes the apoptosis of THP-1-derived macrophages through the CHOP-dependent pathway. *Int J Mol Med* **34**, 886–893, doi:10.3892/ijmm.2014.1833 (2014).
81. Berghofer, B., Haley, G., Frommer, T., Bein, G. & Hackstein, H. Natural and synthetic TLR7 ligands inhibit CpG-A- and CpG-C-oligodeoxynucleotide-induced IFN-alpha production. *J Immunol* **178**, 4072–4079, doi:10.4049/jimmunol.178.7.4072 (2007).
82. Shibata, T. *et al*. Guanosine and its modified derivatives are endogenous ligands for TLR7. *Int Immunol* **28**, 211–222, doi:10.1093/intimm/dxv062 (2016).
83. Boddi, M. *et al*. Hepatitis C virus RNA localization in human carotid plaques. *J Clin Virol* **47**, 72–75, doi:10.1016/j.jcv.2009.10.005 (2010).
84. Gredmark, S., Jonasson, L., Van Gosliga, D., Ernerudh, J. & Soderberg-Naucler, C. Active cytomegalovirus replication in patients with coronary disease. *Scand Cardiovasc J* **41**, 230–234, doi:10.1080/14017430701383755 (2007).
85. Boddi, M. *et al*. HCV infection facilitates asymptomatic carotid atherosclerosis: preliminary report of HCV RNA localization in human carotid plaques. *Dig Liver Dis* **39**(Suppl 1), S55–60, doi:10.1016/S1590-8658(07)80012-0 (2007).
86. Alber, D. G., Powell, K. L., Vallance, P., Goodwin, D. A. & Grahame-Clarke, C. Herpesvirus infection accelerates atherosclerosis in the apolipoprotein E-deficient mouse. *Circulation* **102**, 779–785, doi:10.1161/01.CIR.102.7.779 (2000).
87. Lin, E., Freedman, J. E. & Beaulieu, L. M. Innate immunity and toll-like receptor antagonists: a potential role in the treatment of cardiovascular diseases. *Cardiovasc Ther* **27**, 117–123, doi:10.1111/j.1755-5922.2009.00077.x (2009).

Acknowledgements

The authors thank Chelsea Swallom for editorial assistance. This study is supported by grants from the Natural Science Foundation of China grants (81570274 to J.Y.Z.) and the National Institutes of Health (HL60942, HL81090, and HL123568 to G.P.S.).

Author Contributions

C.L.L., and M.M.S. designed and performed most of the experiment. C.F. generated mouse model. M.L. and K.I. was responsible for mouse lesion and blood characterization. J.Y.Z. was involved in experimental design. G.K.S. performed most of the lesion immunohistochemical analysis. G.P.S. designed the experiments and wrote the manuscript.

Additional Information

Competing Interests: The authors declare that they have no competing interests.

Publisher's note: Springer Nature remains neutral with regard to jurisdictional claims in published maps and institutional affiliations.